

Acoustic-RF Anechoic Chamber Construction and Evaluation

Glenwood Garner III, Jonathan Wilkerson, Michael M. Skeen, Daniel F. Patrick, Ryan D. Hodges, Ryan D. Schimizzi, Saket R. Vora, Zhiping Feng, Kevin G. Gard, and Michael. B. Steer

NC State University, Raleigh, NC, 27695-7911, USA

Abstract — The use of sound as a means to gather information about our environment has been developed with limited scope over the past several decades. The primary application of this technology has been ultrasound and ultrasonic ranging. Recent developments in nonlinear acoustics have proven that two-tone measurements and directional high frequency parametric arrays can extract much more information about the size, shape, and density of objects under inspection. However, acoustic measurements are difficult to make in the laboratory environment due to excessive ambient noise. For these reasons, the Electronics Research Laboratory at NC State University has constructed an acoustic-RF anechoic chamber as a means to make these measurements and further research in nonlinear acoustics and acoustic detection and imaging.

Index Terms — Acoustic Imaging, acoustic materials, acoustic measurements, electromagnetic measurements, electromagnetic propagation.

I. INTRODUCTION

Research in classical ultrasonic acoustics has primarily focused on imaging techniques such as ultrasound that rely solely on orthogonal reflections and measuring time of flight data. Recently, techniques that use two frequencies, and the nonlinear effect of air or other media, have shown promise in gathering even more information about our environment. This information can include not only range and shape data, but also resonance and density measurements. Furthermore, research in this field can improve techniques for air coupled ultrasonic inspection where a large impedance mismatch limits the ability to transmit high-energy signals from one media to another.

The Electronics Research Laboratory (ERL) at NC State University has recently become interested in performing ultrasonic as well as ultrasonic induced electromagnetic experiments. Such experiments in nonlinear two-tone acoustics that exploits the resonant nature of the material under inspection can be of use in landmine and fossil detection and imaging. For these applications, the difference between the two frequencies can provide low frequency excitation, while maintaining the directionality and standoff distance from the target.

In order to measure acoustic, electromagnetic, and acoustically modulated electromagnetic phenomenon, ERL decided to build the first anechoic chamber that attenuates both acoustic and RF energy. An emphasis on measuring life-sized specimens led to a design that measures 8 feet in width, 6 feet in height, and 12 feet long. Furthermore, measurements show that the chamber provides significant insertion and return loss as well as dynamic ranges of 114 dB and 130 dB for acoustic and electromagnetic measurements respectively.

II. ANECHOIC CHAMBER CONSTRUCTION

Overall external chamber dimensions are 96 inches in width, 72 inches in height, and 144 inches in length. Due to the thickness of absorbent materials used in construction, the internal usable dimensions are 76 inches in width, 52 inches in height, and 120 inches in length. Chamber construction began by building a raised floor to provide wire runs to various test equipment located within the chamber. The floor measures 109 inches in width by 156 inches in length and rests on top of 9 4"x4" posts. Starting from the lower most layer, the floor is comprised of one layer 3/4" plywood, one layer cement board, one layer copper mesh, and two layers of 6.0 mm thick Acoustiblok.

The walls and ceiling of the anechoic chamber are all constructed using the same process. Support for the walls is via an extruded aluminum space frame manufactured by 80/20 Inc. The outermost layer of each wall and ceiling panel is comprised of copper mesh, manufactured by TWP Inc.[1], forming a Faraday cage around the entire chamber.

Forming the foundation of each wall and ceiling panel is a layer of 3.0 mm thick Acoustiblok. This high-density rubberized material provides almost 2/3 of the through-wall attenuation above 1.0 kHz [2]. The Acoustiblok sandwiches the copper mesh against the supporting frame and is held in place with 1.5 in. nylon bolts spaced 4 in. apart. At every seam in the Acoustiblok, acoustical sealant and tape is used to further improve soundproofing. Completion of this step allowed the space frame to be erected and application of RF absorbent tiles to begin.

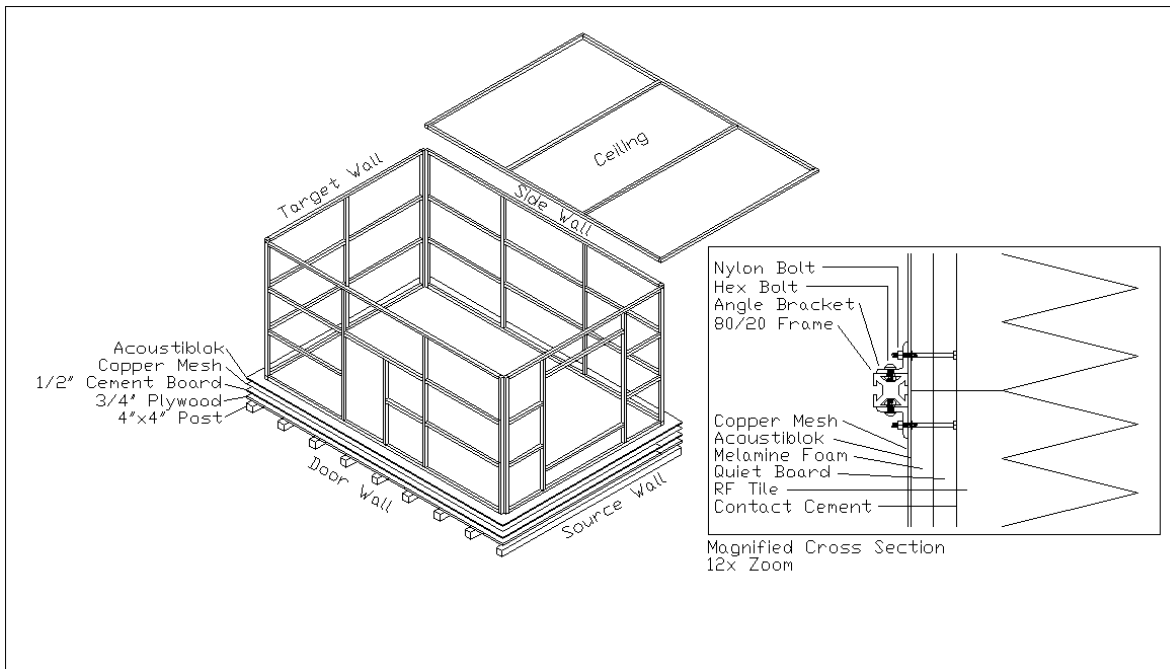


Fig. 1. Exploded view of chamber frame and floor. Magnified cross section shows wall construction detail. The Acoustiblok and copper mesh are held in place with a 0.25 x 1.5 in. nylon flat head bolts and nuts attaching these layers to each angle bracket. The Melamine/Quiet Board panels are held in place with 0.25 x 4 in. nylon carriage bolts. Finally, RF tiles are glued to the Quiet Board using contact cement.

Attached to the inside surface of the Acoustiblok are 2 ft. by 4 ft. panels of QuietBoard glued to Melamine foam, both manufactured by American Micro Industries. Each panel is attached by six nylon bolts and forms the surface to which the RF absorbing foam tiles are glued. At every point where these panels are attached, Acoustiblok sealant is again used to ensure soundproofing.

The innermost layer consists of RF absorbing geometric tiles. Two types of this tile were donated to the ERL, each measuring 2 ft. square. The pyramidal style tile was used in the most sensitive areas such as along the back wall where the most intense energy will accumulate. Eggshell tiles were used to fill in where there were not enough of the previous type. All of the tiles were arranged in a manner that reduced the possibility of generating standing waves under continuous signal generation.

III. ANECHOIC CHAMBER ACOUSTIC CHARACTERIZATION

To evaluate the acoustic performance of the anechoic chamber, experiments were conducted to measure the chamber's insertion and return loss. If the wall were modeled as a two-port network, this would correspond to values for S_{21} and S_{11} respectively.

Transmission measurements were performed at both low frequencies from 0.1-20 kHz, as well as at ultrasonic frequencies from 50-70 kHz. Low frequency signals were generated using a PXI-4461 DAQ and transmitted with an Event Electronics TR-8 Studio Monitor. High frequency signals were generated with a Marconi 2024 signal

generator and transmitted using an 18 in. Audio Spotlight transducer/amplifier combination customized to accept ultrasonic input. Data was recorded using a PXI-5922 high-speed digitizer connected to PCB Piezotronic condenser microphones. For transmission measurements, one microphone inside the chamber recorded the incident sound pressure level, while another outside the chamber recorded the transmitted sound pressure level. Insertion loss in decibels was calculated using [2]

$$L_i = 20 \cdot \log_{10} \left(\frac{P_t}{P_i} \right), \quad (1)$$

where P_t is the transmitted pressure amplitude and P_i is the incident pressure amplitude. The lowest possible sound pressure amplitude that can be measured with our microphones is 6 dB SPL. This noise floor was calculated using [2],

$$X_k = \frac{2}{N} \cdot \sum_{n=0}^{N-1} X_n \cdot e^{-\frac{2 \cdot \pi \cdot i \cdot k \cdot n}{N}}. \quad (2)$$

The discrete Fourier transform was computed at the frequency of interest, over a range of 500,000 time samples and a sampling rate of 500 kHz. The maximum sound pressure amplitude that can be generated with our transmitters is 120 dB SPL. This gives an acoustic dynamics range of 114 dB SPL.

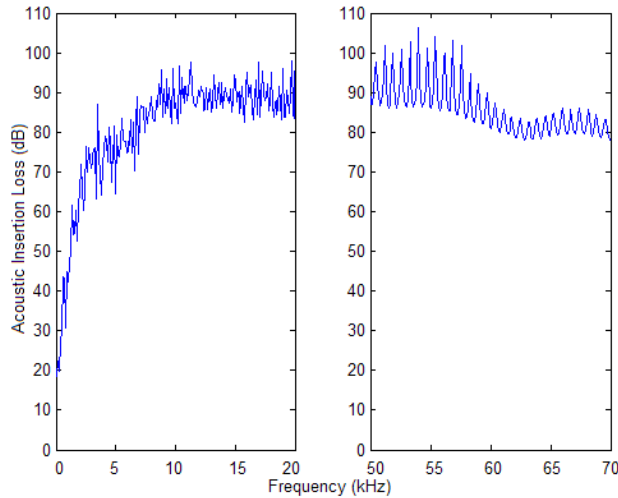


Fig. 2. Acoustic insertion loss of back wall of anechoic chamber. Above 50 kHz where higher power signals can be generated, the periodicity of the attenuation indicates that a resonance is being generated.

Reflection measurements were also performed at low frequencies from 0.1-20 kHz and high frequencies from 50-70 kHz. For reflection measurements, all signals were generated using a PXI-4461 DAQ. The low frequency signals were transmitted using the Event Electronics TR-8 Studio Monitors while the high frequency signals were transmitted using the Audio Spotlight. One microphone recorded the incident sound pressure amplitude while another recorded the reflected sound pressure amplitude. Significant amounts of acoustic shielding were required to isolate the reflected microphone from the incident one, as well as using a geometry that separated the incident and reflected microphones by approximately 1.0 meter. The incident and reflected microphones were aligned using a laser so that they each resided within the loudest portion of the sound beam. Return loss in decibels was then calculated using

$$L_r = 20 \cdot \log_{10} \left(\frac{P_r}{P_i} \right), \quad (3)$$

where P_r is the reflected pressure amplitude and P_i is the incident pressure amplitude. Given the increased path distance for reflection measurements, a correction was made to account for free space path loss as the sound wave traveled from the incident microphone to the reflected microphone.

VI. ANECHOIC CHAMBER RF CHARACTERIZATION

Both transmission and reflection measurements were taken using S_{21} parameters. An HP8510C network analyzer was used to generate a 0.0 dBm signal at Port 1 to an ETS-Lindgren 3164-03 horn antenna through a frequency range of several GHz. A copper conical-hat receiving antenna connects to Port 2.

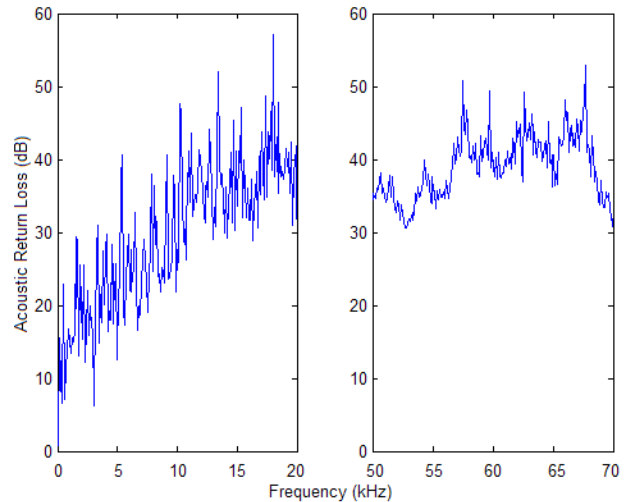


Fig. 3. Acoustic return loss of back wall of anechoic chamber.

For insertion loss measurements, the transmitting antenna points directly to the receiving antenna at a distance of 1.55 meters with polarization aligned. A calibration was initially performed to account for beam spreading across this range. Two S_{21} measurements are made, one with the receive antenna outside the chamber, and one with both antennas inside the chamber at the same distance. The first measurement is divided by the second to obtain a transmission coefficient.

Initial transmission measurements only captured -80 dBm noise with a 0.0 dBm input. The insertion loss was so great that the receiving antenna outside the chamber picked up only noise. To increase the dynamic range, an Ophir 5164 28-watt RF Amplifier was placed at Port 1 to amplify the transmitted signal by 40 dB. In plotting the data, 40 dB is added to account for amplification.

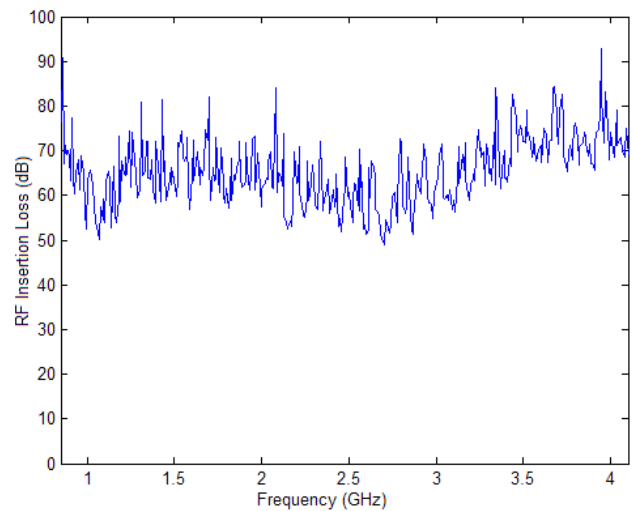


Fig. 4. RF insertion loss of the back wall of the anechoic chamber averages 65 dB.

V. CONCLUSION

For return loss measurements, the transmitting antenna points toward the back wall at a distance of 0.86 m, while the receiving antenna is aligned to receive the signal following the most direct ray bounce at a distance of 1.58 m from the wall. A thick stack of RF absorber is then placed between the two antennas to isolate side lobe interference. The S_{21} measurement is then divided by a calibrating S_{21} measurement to account for antenna gain and beam spreading of the two antennas. The calibrating measurement was performed with the transmit and receive antennas placed at a distance of $0.86 + 1.58 = 2.44$ m. The frequency range of the conical antenna has a large bandwidth while the horn antenna has a frequency range of 0.4 – 6 GHz.

The RF insertion loss averages approximately 65 dB. This is more than enough to provide for the safety of any persons near the anechoic chamber. While the reverse measurement was not taken directly, outside signals should not affect measurements inside the chamber in any appreciable manner.

RF return loss oscillates between 20 – 40 dB, indicating an adequate lack of reflection for our future measurements. The oscillation corresponds to a half wavelength of approximately 30 cm at 50 MHz, which is approximately the thickness of our chamber wall. Furthermore, the comparative drop in return loss around 2.6 GHz corresponds to a drop in the gain of our transmitting antenna in the same range. This drop in antenna gain should theoretically be cancelled out in our calibration, but a nonlinearity in electromagnetic interaction with the chamber wall may leave some residual effects.

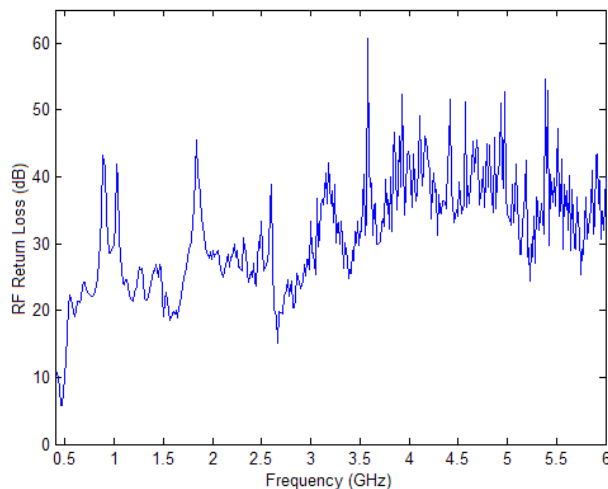


Fig. 5. The RF return loss averages approximately 30 dB. Oscillations may indicate a chamber wall resonance, and the dip at 2.6 GHz corresponds to a drop in antenna gain.

Measurements show that the ERL anechoic chamber significantly attenuates both transmitted and reflected acoustic and RF energy. For acoustic measurements, the chamber offers up to 100 dB insertion loss and 45 dB return loss. Furthermore, the ERL system has been shown to achieve an acoustic dynamic range of over 110 dB. RF measurement data show insertion loss of up to 90 dB, and a return loss of up to 50 dB. Return loss data for the RF absorbent foam from the manufacturer indicates that the foam itself should have higher return loss than the measured data for the ERL anechoic chamber. Other measured data collected indicated that interactions between the two antennas used for measurement may have been interacting and affecting the measured return loss performance of the chamber. It is possible with a higher level of antenna isolation the measured performance would improve.

ACKNOWLEDGEMENT

This material is based upon work supported by the U. S. Army Research Laboratory and the U. S. Army Research Office under grant number W911NF-07-1-0004.

REFERENCES

- [1] R.W. Evans, *Design Guidelines for Shielding Effectiveness, Current Carrying Capability, and the Enhancement of Conductivity of Composite Materials*, National Aeronautics and Space Administration., Tec-Masters, Inc, Contractor Report 4784, August 1997.
- [2] R. Stoessel, *Air-Coupled Ultrasound Inspection as a New Non-Destructive Testing Tool for Quality Assurance*, Dissertation, University of Stuttgart, 2004.